Applied Thermal Engineering 100 (2016) 55–61

Contents lists available at ScienceDirect

Applied Thermal Engineering

journal homepage: www.elsevier.com/locate/apthermeng

Research Paper

Numerical analysis of turbulent round jet impingement heat transfer at high temperature difference

Taotao Zhou, Dong Xu, Jing Chen, Changmin Cao, Taohong Ye *

Department of Thermal Science and Energy Engineering, University of Science and Technology of China, Hefei 230027, China

HIGHLIGHTS

- Validation of the V2F turbulent model is performed.
- Effect of the density and thermal properties on heat transfer is quantitatively studied.
- Modified correlations for impingement heat transfer at high temperature difference.

ARTICLE INFO

Article history:
Received 21 August 2015
Accepted 5 February 2016
Available online 13 February 2016

Keywords:
Jet impingement
Heat transfer
High temperature difference
Round nozzle

ABSTRACT

Heat transfer of round jet impingement at high temperature difference was numerically investigated with V2F turbulent model. Validation of the model was evaluated against available experimental data. Effect of the density and thermal properties on heat transfer was studied. Numerical results show that the decrease of density leads to decrease of the heat transfer coefficient while the increase of each thermal property leads to increase of the heat transfer coefficient. Meanwhile, Nusselt number is found to be independent of the temperature difference and can be calculated from the correlation at low temperature difference on the condition that the jet inlet temperature is selected as the qualitative temperature. Correlation proposed by earlier researcher is then modified for impingement heat transfer at high temperature difference.

1. Introduction

Jet impingement is widely utilized in industrial applications for its enhanced heat transfer rate, such as drying of textile and paper products, electronics cooling, cooling of gas turbine blades and outer wall of the combustion chamber, heating and cooling of steel sheets. In many of these cases, the temperature difference ranges from only a few dozen degrees to more than one thousand degrees. Many factors affecting the impingement heat transfer have been investigated extensively in the last decades, such as the jet nozzle geometry [1–3], jet Reynolds number [4–8], the ratio of the jet-to-plate distance to the nozzle exit diameter [9–12], jet impinging angle [1,7,13–19], entrainment effects [20–24], swirl of the jet flow [25–29], and surface roughness [30,31]. In addition, plenty of correlations for impingement heat transfer have been proposed [32] and the general form of these correlations is: $Nu = f(Re, Pr, geometry)$, where Nu is Nusselt number, Re is jet Reynolds number, and Pr is Prandtl number.

However, most investigation focused on impingement flows with a small temperature difference between the jet and the target surface, only a few research has been carried out at high temperature difference. Experimental results of Refs. 3 and 33 showed that Martin's [34] correlation fits well at low temperature difference, while the difference between experimental data and Martin's [34] correlation gets significant with the increase of temperature difference. A new correlation with temperature correction was suggested but the correlation was claimed only effective under certain conditions. Shi [35] predicted the impingement heat transfer at the temperature difference between 10 °C and 200 °C with RSM turbulent model and a comparison was made between the Nusselt number distributions under different definitions. Jensen and Walther [36] numerically analyzed the effect of jet turbulence intensity on the impingement heat transfer at high temperature difference with V2F model and proposed a correlation between stagnation point Nusselt number, Reynolds number and turbulence intensity.

The density and thermal properties of jet vary greatly at high temperature difference, which could significantly affect the heat transfer rate and is the reason why it differs from the condition at low temperature difference. The motivation of the present research is to investigate and develop the correlations of round jet impingement heat transfer at high temperature difference. The effect of density and thermal properties on heat transfer is investigated numerically with V2F turbulent model at first. Then the heat transfer correlation at high temperature difference is proposed according to the numerical results.

* Corresponding author. Tel.: +86 13966707461; fax: 86-0551-3603048.
E-mail address: thye@ustc.edu.cn (T. Ye).

http://dx.doi.org/10.1016/j.applthermaleng.2016.02.006
1359-4311/

2. Physical model and numerical methods

2.1. Brief description of impinging turbulent round jet flow

The configuration of single impinging round jet flow investigated in this work is shown in Fig. 1, the jet inlet diameter D is 0.01m, and the non-dimensional distance H/D is 2. The jet Reynolds number varies from 4000 to 12,000. The jet temperature at the inlet T_{jet} varies from 298.15 K to 873.15 K, the environment temperature is set equal to the jet inlet temperature, and the wall temperature T_{wall} is 273.15 K. The pressure in the system is 1 atm. The heat transfer rate is usually described by Nusselt number, $Nu = hD/\lambda$, $h = q/(T_{wall} - T_{jet})$, where h is the heat transfer coefficient, λ is thermal conductivity, q is the heat transfer rate, respectively.

2.2. Governing equations and turbulence model

Ignoring the effect of radiation and adopting the Favre average [37] (mass-weighted average), the steady-state averaged Navier–Stokes equations are as follows:

$$\frac{\partial}{x_i}(\bar{\rho}\tilde{u}_i) = 0 \tag{1}$$

$$\frac{\partial \bar{\rho}\tilde{u}_i\tilde{u}_j}{x_j} = -\frac{\partial \bar{P}}{x_i} + \frac{\partial}{x_i}\left(\bar{\tau}_{ij} - \overline{\rho u_i'' u_j''}\right) \tag{2}$$

$$\frac{\partial \bar{\rho}\tilde{u}_i\tilde{h}_e}{x_i} = \frac{\partial}{x_i}\left(\lambda\overline{\frac{\partial T}{x_i}} - \overline{\rho u_i'' h_e''}\right) + \tilde{u}_i\frac{\partial \bar{P}}{x_i} + \overline{\tau_{ij}\frac{\partial u_i}{x_j}} \tag{3}$$

where ρ is density, P is pressure in the system. u_i is the velocity component along the i_{th} coordinate (x_i) direction. h_e is enthalpy, T is temperature and τ_{ij} is viscous stress tensor $\left(\tau_{ij} = -\frac{2}{3}\mu\frac{\partial u_k}{\partial x_k}\delta_{ij} + \mu\left(\frac{\partial u_i}{\partial x_j} + \frac{\partial u_j}{\partial x_i}\right)\right)$. μ is dynamic viscosity and δ_{ij} is the Kronecker symbol. The superscript "—" represents Reynolds averaged values. The superscript "~" represents mass-weighted averages.

In this work Reynolds stresses are closed by V2F model [38,39] and enthalpy turbulent fluxes are closed using the classical gradients assumption:

$$-\overline{\rho u_i'' u_j''} = \mu_t\left(\frac{\partial \tilde{u}_i}{\partial x_j} + \frac{\partial \tilde{u}_j}{\partial x_i} - \mu_t\frac{\partial \tilde{u}_k}{\partial x_k}\delta_{ij}\right) - \frac{2}{3}\bar{\rho}k \tag{4}$$

$$-\overline{\rho u_i'' h_e''} = \frac{\mu_t}{Pr_t}\frac{\partial \tilde{h}_e}{\partial x_i} \tag{5}$$

where k is turbulent kinetic energy $\left(k = \widetilde{u_i'' u_i''}/2\right)$, μ_t is the turbulent dynamic viscosity $\left(\mu_t = \bar{\rho}C_\mu\overline{v''^2}\tilde{T}\right)$, Pr_t is turbulent Prandtl number. Unlike $k-\varepsilon$ model, V2F model estimates the turbulent dynamic viscosity by the velocity component in the wall-normal direction and directly calculates all the values in the viscous sublayer, which improve the computational accuracy and better describe the anisotropy of turbulent flows in regions near the wall. It should be noted that the RNG $k-\varepsilon$ model [40], the shear-stress transport (SST) $k-\omega$ model [41] and the Reynolds stress model (RSM) [42–44] are also used to compare the performance of different turbulence models in impinging round jet heat transfer.

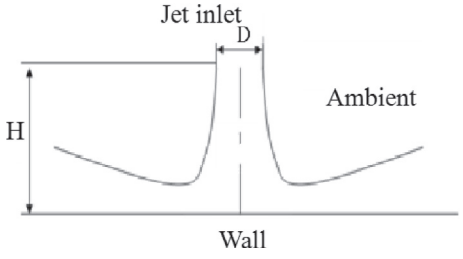

Fig. 1. Impinging jet configuration.

2.3. Density and thermal properties

The fluid used in the paper is air. The maximum Mach number of the flow in this work is below 0.3, so the flow can be treated as incompressible. The density and thermal properties are considered only changing with temperature. Density is calculated using the incompressible ideal gas law: $\rho = P\Big/\left(\frac{RT}{M}\right)$, where R is universal gas constant and M is molecular weight of gas. Dynamic viscosity is calculated by Sutherland law: $\mu = \mu_0\left(\frac{T}{T_0}\right)^{3/2}\frac{T_0+S}{T+S}$, isobaric specific heat capacity c_p is calculated using piecewise polynomial correlations and thermal conductivity λ is calculated using kinetic molecular theory.

2.4. Mesh and boundary conditions

On the condition that the impinging round jet flow is assumed axisymmetric, the computational domain is simplified to a two-dimensional configuration which is $2D \times 10D$ in the vertical and horizontal directions respectively. The generated structured mesh is shown in Fig. 2, which is refined in the near wall region, near nozzle region and jet shear layer. The solution of a turbulent fully developed pipe-flow simulation is used for prescribing the inflow averaged velocity profile and all the turbulent parameters of the impinging jet. The jet inlet temperature is T_{jet}. The target surface is considered to be a no-slip wall with a fixed temperature of 273.15 K. The outlet boundary and the upper boundary are considered as pressure outlet boundary.

2.5. Discretization and algorithm

The numerical study is carried out using the commercial CFD software Fluent. SIMPLE algorithm is applied to solve the couple of pressure and velocity and the finite volume method is adopted to discrete the governing equations. The discretization of convection term is imposed with second-order upwind interpolation scheme and the discretization of diffusion term is imposed with second-order central difference scheme.

3. Results and discussion

3.1. Validation of grid independency

V2F model does not employ any wall model and the mesh near the wall must be sufficiently fine. To examine grid independency, computations of impingement at the jet Reynolds number of 8000 and the temperature difference of $\Delta T = T_{jet} - T_{wall} = 25K$ are performed on four consecutively refined grids, which are 165×300 cells (Mesh1), 210×300 cells (Mesh2), 270×300 cells (Mesh3), and 310×300 cells (Mesh4) in the vertical and horizontal directions, respectively. The local Nusselt number distributions are shown in Fig. 3. The dimensionless wall distances $y^+ = y\sqrt{\tau_w\rho}/\mu$ (y is the normal distance of the first mesh cell to the wall, τ_w is the wall shear stress) are 5.62, 1.75, 0.59, 0.14, respectively. Mesh3 and Mesh4 give almost the same distribution, the maximum difference is 3% between results predicted by Mesh2 and Mesh4, while the maximum difference is 9% between Mesh1 and Mesh4. So Mesh3 is considered